

Chemistry A European Journal

 **Chemistry
Europe**
European Chemical
Societies Publishing

Accepted Article

Title: Regioselective Synthesis of 4-Aryl-1,3-dihydroxy-2-naphthoates through 1,2-Aryl-migrative Ring Rearrangement Reaction and Their Photoluminescence Properties

Authors: Hikaru Yanai, Teru Kawazoe, Nobuyuki Ishii, Bernhard Witulski, and Takashi Matsumoto

This manuscript has been accepted after peer review and appears as an Accepted Article online prior to editing, proofing, and formal publication of the final Version of Record (VoR). This work is currently citable by using the Digital Object Identifier (DOI) given below. The VoR will be published online in Early View as soon as possible and may be different to this Accepted Article as a result of editing. Readers should obtain the VoR from the journal website shown below when it is published to ensure accuracy of information. The authors are responsible for the content of this Accepted Article.

To be cited as: *Chem. Eur. J.* 10.1002/chem.202101459

Link to VoR: <https://doi.org/10.1002/chem.202101459>

WILEY-VCH

FULL PAPER

Regioselective Synthesis of 4-Aryl-1,3-dihydroxy-2-naphthoates through 1,2-Aryl-migrative Ring Rearrangement Reaction and Their Photoluminescence Properties

Hikaru Yanai,*^[a] Teru Kawazoe,^[a] Nobuyuki Ishii,^[a] Bernhard Witulski,*^[b] and Takashi Matsumoto*^[a]

- [a] Dr. Hikaru Yanai, Teru Kawazoe, Nobuyuki Ishii, Prof. Dr. Takashi Matsumoto
School of Pharmacy, Tokyo University of Pharmacy and Life Sciences
1432-1 Horinouchi, Hachioji, Tokyo 192-0392, Japan.
E-mail: yanai@toyaku.ac.jp (HY), tmatsumo@toyaku.ac.jp (TM). Twitter handle: @TUPLS_seizo
- [b] Prof. Dr. Bernhard Witulski
Laboratoire de Chimie Moléculaire et Thio-organique, CNRS UMR 6507
ENSICAEN & UNICAEN, Normandie Univ.
6 Bvd Maréchal Juin, Caen, 14050, France.
E-mail: bernhard.witulski@ensicaen.fr

Supporting information for this article is given via a link at the end of the document.

Abstract: 4-Aryl-1,3-dihydroxy-2-naphthoates having the less accessible 1,2,3,4-tetrasubstituted naphthalene scaffold and that show photoluminescence emission from solid state as well as in solutions, were selectively synthesized from brominated lactol silyl ethers through the 1,2-aryl-migrative ring rearrangement reaction.

Introduction

Structural diversity of polyketide natural products and their unique biological activities have attracted much attention over the past 100 years.^[1] For example, aromatic polyketides, which are produced through biosynthetic pathways catalysed by type II polyketide synthase (PKS) in bacteria,^[2] are still regarded as challenging targets for chemical synthesis because of difficulties in the selective construction of highly-substituted polycyclic aromatic scaffolds.^[3] As shown in Figure 1, in the biosynthesis of the antibiotic actinorhodin,^[4] the acyclic intermediate **INT-1** is initially converted to the monocyclic intermediate **INT-2**, which produces a series of secondary tricyclic metabolites including actinorhodin.

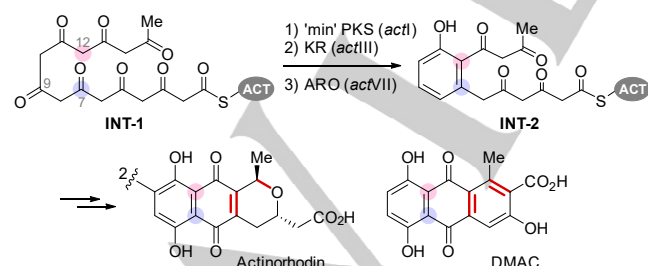
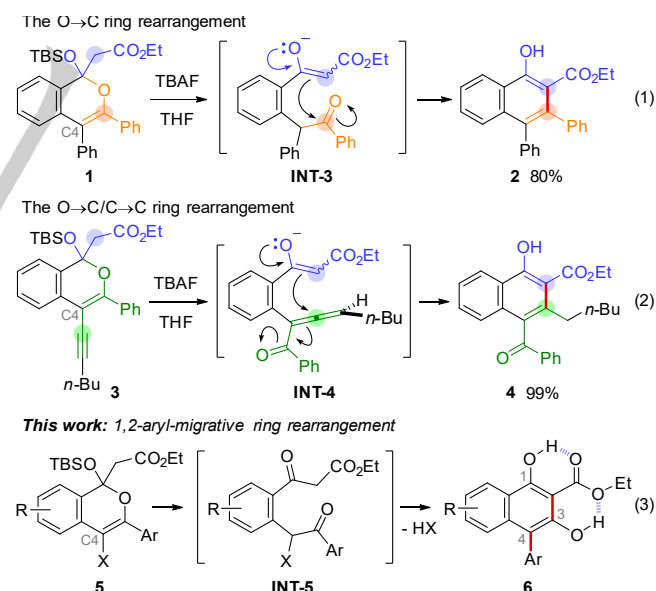


Figure 1. Biosynthetic pathway of actinorhodin and related polyketides.

The conformationally restricted **INT-2**, that promotes follow-up ring-closures, has prompted us to develop related sequential reactions for poly-substituted aromatics.^[5,6] In our early achievement, naphthol **2** was synthesised by treating lactol silyl

ether **1** with suitable fluoride sources (Eqn. 1).^[7] This O→C ring rearrangement reaction proceeded via a desilylative ring-opening that was followed by an intramolecular aldol reaction of the thermodynamically favoured keto-enolate **INT-3**. Under similar conditions, the C4-alkynyl substrate **3** selectively gave naphthalene **4** bearing a different substituent pattern on the consecutive 1–4 positions (Eqns. 1 vs 2).^[8] In this case, the intramolecular Michael reaction of allenyl ketone **INT-4** was proposed being the ring-closing step (O→C/C→C ring rearrangement reaction).



Such a 'ring rearrangement' strategy using a lactol silyl ether scaffold has the following remarkable features: (1) a synthetic protocol for starting lactol derivatives with latent reactive functionalities is highly reliable, (2) a variety of C4-substituents on the isochromene backbone bring structural diversity of the naphthalene substituents (Eqn. 1), (3) the cyclisation mode is also switchable by changing the C4-substituents (Eqns. 1 vs 2), and (4) the isolation of lactol silyl ethers allows detailed screening and optimisation of the ring rearrangement conditions. Considering

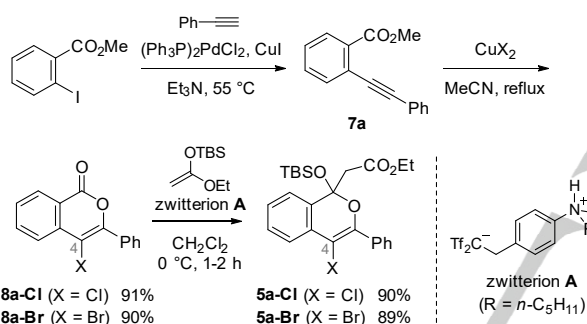
FULL PAPER

the importance of natural product-like compounds having a polycyclic aromatic scaffold in the fields of medicinal and material chemistry,^[9] challenging and less accessible 1,2,3,4-tetrasubstituted naphthalenes are highly attractive targets.^[10,11] In this paper, we report that the C4-halogenated substrate **5** selectively gives the 4-aryl-1,3-dihydroxy-2-naphthoate **6** (Eqn. 3) via the α -haloketone intermediate **INT-5**. We also found that the rigid molecular framework found in **6** with its two characteristic intramolecular H-bonds became a potent molecular motif for solution and solid-state fluorescent materials.

Results and Discussion

Development of a novel cascade reaction for 4-aryl-1,3-dihydroxy-4-naphthoates

We started our investigation with the synthesis of the C4-halogenated lactol silyl ethers **5a-X** (X = Cl, Br, I). According to a reported procedure,^[12] 4-chloro- and 4-bromo-1*H*-isochromen-1-ones **8a-Cl** and **8a-Br** were prepared from methyl *o*-iodobenzoate over two steps (Scheme 1). By applying the zwitterion catalyst **A** developed by us,^[7,13] the addition reaction of a ketene silyl acetal to the lactones gave **5a-X** in excellent yields.



Scheme 1. Preparation of 4-halogenated lactol silyl ethers.

With **5a-X** in our hand, its reactivity was examined. Unfortunately, applying TBAF-induced conditions^[7] to **5a-Cl** led to an intractable mixture of products. On the other hand, the E1 product **9a-Cl** was obtained after heating at 70 °C in acetic acid (Table 1, entry 1).^[14] Interestingly, in the presence of NaOAc, **9a-Cl**, that now was *in situ* generated from **5a-Cl** (reaction followed by TLC), was converted to the unexpected product **6a**. The latter was, however, also accompanied by the expected product **10a-Cl** dependent on the amount of NaOAc used (Table 1, entries 2-4). The reaction path to **6a** can be best explained by a 1,2-aryl-migration process. We noted that in a traditional synthesis of 1,3-dihydroxy-2-naphthoates through the C-acylation of malonates with acid chlorides followed by cyclisation in the presence of acid promoters, which was reported by Meyer and Bloch in 1945,^[15a] the 4-substituted derivatives were not obtained effectively.^[15b-d] Consequently, our finding motivated to optimise this 1,2-aryl-migrative rearrangement cascade. Eventually, we found that replacing the chlorine atom by a bromine atom caused a significant improvement of the yield of **6a**: the reaction of **5a-Br** in an AcOH/NaOAc mixture gave **6a** in 96% yield. Notably, now the formation of **10a-Br** was suppressed significantly (**10a:6a** = 3:97) (Table 1, entry 5). However, the reaction with the thermally less

stable iodinated substrate **5a-I**^[7] was not fruitful at all (Table 1, entry 6).

Table 1. Reactions of C4-halogenated lactol silyl ethers.

Entry	X	NaOAc (Equiv.)	Time (h)	Yield ^[a] (%)			Ratio ^[b] (9a:10a:6a)
				9a	10a	6a	
1	Cl	None	2.5	93	0	0	100 : 0 : 0
2	Cl	1	2.5	92	-	-	100 : 0 : 0
3	Cl	10	23	-	17	60	11 : 17 : 72
4	Cl	20	23	-	22	59	0 : 33 : 67
5	Br	20	4	-	-	96	0 : 3 : 97
6	I	20	3	complex			-

[a] Isolated yield. [b] Determined by ¹H NMR analysis of crude material.

The scope of this new ring rearrangement cascade that is terminated by an 1,2-aryl migration was examined (Figure 2).

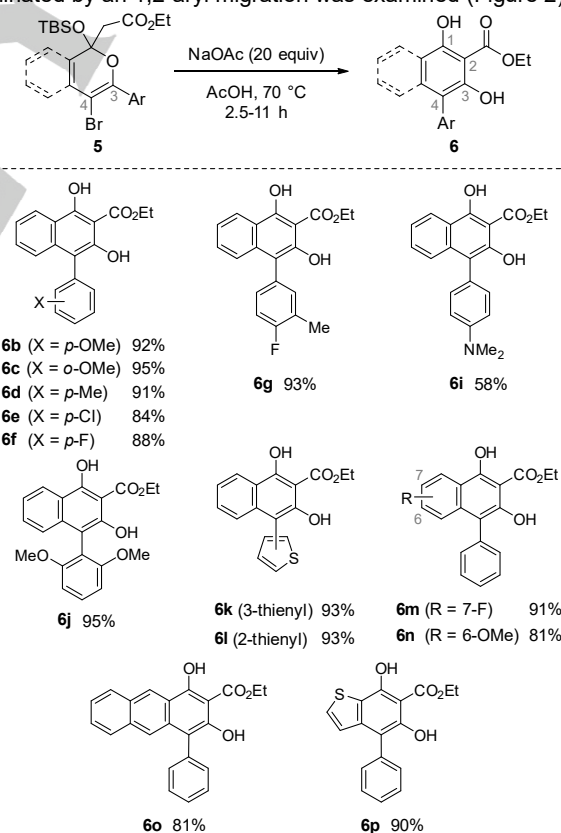
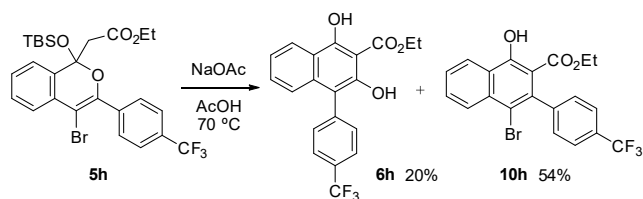


Figure 2. Ring rearrangement reaction of brominated lactol silyl ethers.

The *p*- and *o*-methoxyphenyl substrates **5b**, **5c** and the *p*-tolyl substrate **5d** gave the corresponding products **6b-d** in excellent

FULL PAPER

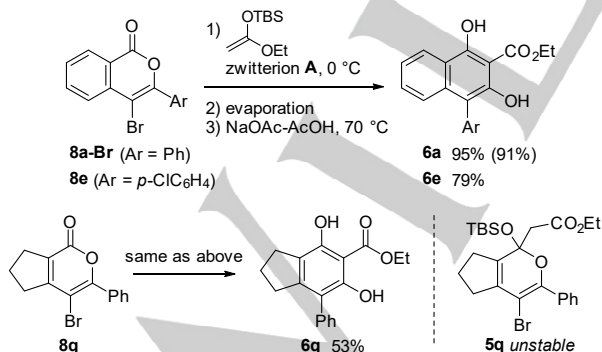
yields. Likewise, the substrates **5e–5g** bearing slightly electron-deficient aryl groups were successfully converted to the desired products **6e–6g**. The *p*-dimethylamino derivative **6i** was isolated in 58% yield despite of the used acidic conditions. In addition, the highly congested naphthoate **6j**, was obtained in 95% yield. The 2- and 3-thienyl substrates **5k** and **5l** gave the corresponding products **6k** and **6l**, respectively. Substitution of the isochromene backbone did not affect the reaction outcome to give **6m** and **6n** in good to excellent yields. In addition, a selective synthesis of the anthracene **6o** as well as the benzothiophene **6p** was achieved. The reaction with **5h** bearing a strongly electron-withdrawing CF₃ group deserves special notice: 4-bromonaphthalene **10h** was obtained as the major product (54% yield) together with **6h** that was obtained now in 20% yield only (Scheme 2).



Scheme 2. Reaction of **5h** bearing a strongly electron withdrawing CF₃ group.

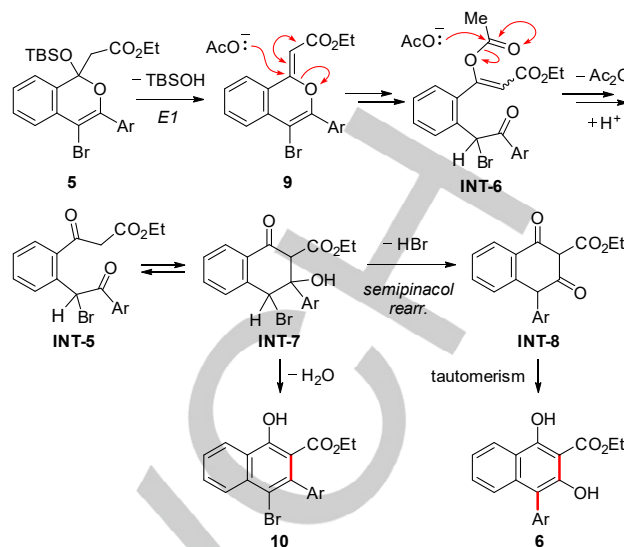
These results imply that the 1,2-aryl migration becomes more favourable with increasing electron-donating character of the migrating aryl group. Despite such a limitation, the present reaction is still promising for the selective formation of a wide range of 4-aryl-1,3-dihydroxy-2-naphthoates.

The one-pot conversion of the bromolactones **8** was alternatively possible (Scheme 3). As a result, the desired naphthalenes **6a** and **6e** were obtained in high yields from **8a–Br** and **8e**, respectively. Note that **6a** was obtained without considerable changes of the yield in a gram-scale reaction using **8a–Br**. This one-pot protocol enables to avoid the isolation of unstable lactol silyl ethers. Although lactol silyl ether **5q** derived from **8q** was not isolable, biphenyl **6q** was obtained in 53% yield from **8q** by applying the one-pot protocol.



Scheme 3. One-pot synthesis of poly-substituted naphthalene and biphenyl. The yield of the gram-scale synthesis of **6a** is shown in parentheses.

A plausible mechanism for the present cascade reaction is shown in Scheme 4.



Scheme 4. Plausible reaction pathways.

Considering the finding that NaOAc is essential for the molecular transformation of **9**, the acetate ion serves here as a nucleophile to generate **INT-6** – a vinylogue of acid anhydride. Sequential intramolecular aldol reaction of α -bromoketone **INT-5** followed by an acid-mediated semipinacol rearrangement are most likely reaction steps.^[16] 4-Bromonaphthalene **10** that is observed in some cases, especially with **5h** bearing a *p*-(trifluoromethyl)phenyl group, is generated through the dehydration of **INT-7**. If the substrate has less reactive electron deficient C3-aryl groups such as **5h**, the dehydration yielding **10** becomes a major path. On the other hand, in most cases, the semipinacol process causes the 1,2-aryl-migration to give the 1,3-dihydronaphthoates **6** selectively. In other words, the **6/10** selectivity reflects the relative rate difference between the 1,2-aryl migration and the dehydration step.

Solid State and Solution Phase Structures

The molecular structure of **6a** was undoubtedly proven by single-crystal X-ray diffraction study.^[17] As shown in Figure 3A, the structure of **6a** and its molecular geometry suggested twofold intramolecular H-bonds (O1–H...O3 and O2–H...O4). Such characteristic bonding was successfully visualized by Bader's Quantum Theory of Atoms in Molecules (QTAIM) analysis^[18] using the DFT-optimized geometry and wave function (Figure 2B). The corresponding bond paths and bond critical points (BCPs) within a reasonable range of QTAIM parameters, including the electron density (ρ_{BCP}) and the Laplacian ($\nabla^2\rho_{\text{BCP}}$), as the O–H...O interaction were computed.^[19] The delocalization index (DI) of the O–H...O interactions,^[20] which may be regarded as a covalent bond order, are 0.101 (for BCP 1) and 0.073 (for BCP 2), respectively.

FULL PAPER

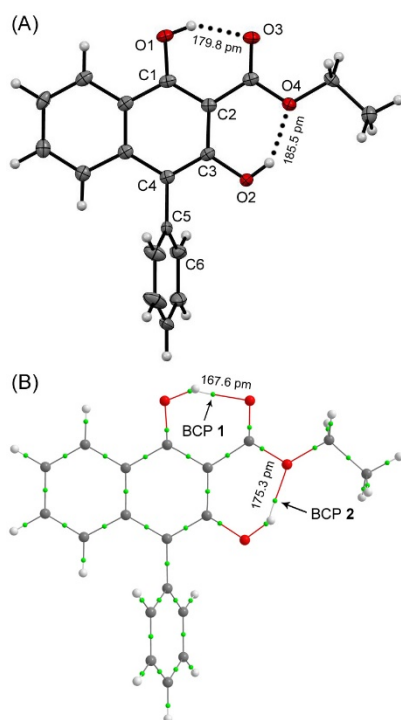


Figure 3. (A) ORTEP drawing of **6a**. Twisting angle around C4-C5 biaryl bond axis was 81.8°. H-atoms attached by calculation in the refinement process. (B) QTAIM view of **6a**. ρ_{BCP1} , 0.333 $\text{e} \text{ \AA}^{-3}$, ρ_{BCP2} , 0.260 $\text{e} \text{ \AA}^{-3}$; $\nabla^2 \rho_{\text{BCP1}}$, +3.784 $\text{e} \text{ \AA}^{-5}$, $\nabla^2 \rho_{\text{BCP2}}$, +3.680 $\text{e} \text{ \AA}^{-5}$ (BCPs are shown by green sphere).

This twofold H-bonding should be considered of being not only present in the solid state but also in the solution phase. For example, in the ^1H NMR analysis of **6a** in CDCl_3 , the singlets for the hydrogen atoms of the C1- and C3-phenolic OH groups are found at 11.61 and 9.28 ppm respectively; and the chemical shifts were not changed significantly by changing the concentration of **6a**. Such a twofold intramolecular H-bonding situation was also found in the X-ray structures of **6d**, **6f**, **6i**, **6j**, **6k**, **6m**, and **6p** obtained from single crystal structure analysis (Figure 4 and Supporting Information).

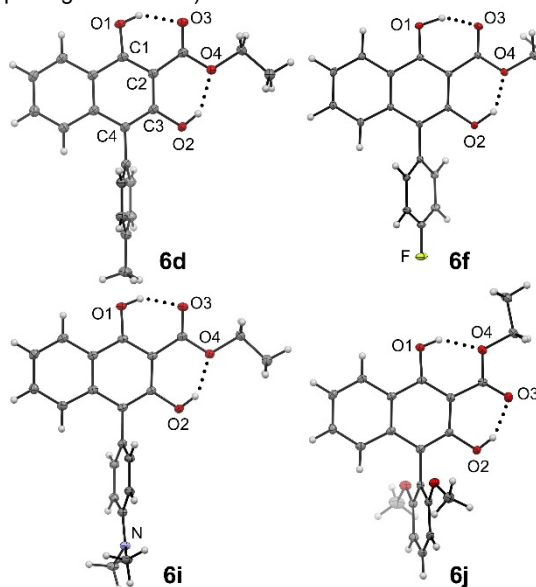


Figure 4. ORTEP drawings of **6d**, **6f**, **6i**, and **6j**.

Photophysical properties

Although the photophysics of 1- and 3-monohydroxy-2-naphthoates found so far little interest in the literature,^[21] we recognized that the 1,3-dihydroxy-2-naphthoate products showed bright PLE from the solid state as well as in solutions. Photophysical data of selected compounds (4-phenyl compounds **6a-f**, **6i**, **6m** and thienyl analogue **6k**) that all show a bright PLE from the solid state and in solution are listed in Table 2, and representative UV-Vis absorption and PLE solution spectra are compiled in Figure 5 (see, Supporting Information for the complete data and spectra sets).

The solution UV-Vis absorption spectra of **6** are characterised by a broad low-energy charge-transfer band in the 325–450 nm region. In a series of 4-phenyl-1,3-dihydroxy-2-naphthoates **6a**, **6b**, **6d-f** bearing *p*-substituents on the phenyl group, the band maxima are slightly red-shifted with increasing donor strength induced by the substituent. Bathochromic shifts, though more pronounced, were also found in the PLE spectra of this series where the emission bands cover the 420–650 nm region. The corresponding Stokes shifts have values of 4200–4700 cm^{-1} . In addition, the Stokes shifts correlated very well with the Hammett–Taft substituent parameter σ_R of the substituents (H, *p*-OMe, *p*-Me, *p*-Cl, *p*-F) on the 4-phenyl group.^[22] This strongly implies the underlying intramolecular charge transfer (ICT) character associated with the longest wavelength absorption and emission bands (Insert of Figure 5). That is, the 4-phenyl-1,3-dihydroxy-2-naphthoates **6a**, **6b**, **6d-f** resemble a considerable ‘push-pull’ system capable for ICT in the excited state. Here, the *p*-substituted phenyl group acts as an electron donor and the naphthoate moiety serves as an electron acceptor. Notably, the *o*-methoxyphenyl derivative **6c** showed similar PLE, but the 2,6-dimethoxyphenyl derivative **6j** was not so. Such results suggest that electronic communication in ground and Franck–Condon excited states seems still to be effective despite the partially twisted nature around the C–C bond axis between the naphthalene backbone and the phenyl substituent. An exception is the fully twisted and ‘locked’ case of **6j**, where its average twist angle is increased (ideally 90°) in comparison to **6c** that is more conformationally flexible around the biaryl bond axis.^[23]

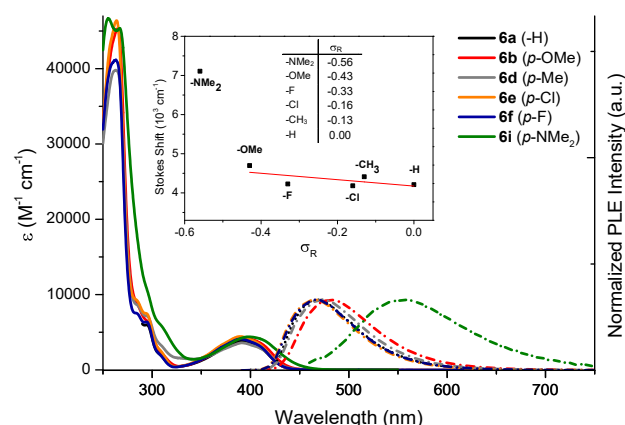
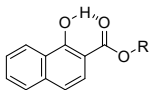
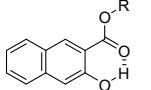
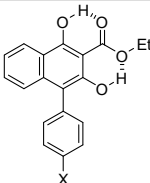
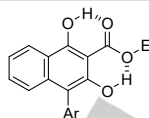
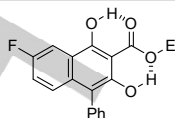


Figure 5. Overlay of UV-Vis absorption spectra (solid lines) and PLE spectra (dashed lines) of the *p*-substituted phenyl naphthoates **6a**, **6b**, **6d-f**, and **6i** in CH_2Cl_2 (10^{-5} M). Insert: Correlation of Stokes shift versus Hammett–Taft substituent parameter σ_R .

FULL PAPER

Table 2. Photophysical data of selected compounds **6**

			6a (X = H) 6b (X = OMe) 6d (X = Me) 6e (X = Cl) 6f (X = F) 6i (X = NMe ₂)			6c (Ar = <i>o</i> -MeOC ₆ H ₄) 6k (Ar = 3-thienyl)	6m
Comp.	Solution ^[a] $\lambda_{\text{max}}^{\text{abs}}$ (nm)	Solution ^[a] ϵ (M ⁻¹ cm ⁻¹)	Solution ^[a] $\lambda_{\text{max}}^{\text{em}}$ (nm)	Solid $\lambda_{\text{max}}^{\text{em}}$ (nm)	Solution ^[a] Stokes shift (cm ⁻¹)	Solution ^[b] ϕ_F	Solid ^[c] ϕ_F
6a	391	3840	468	477	4210	0.39	0.33
6b	393	4320	482	475	4700	0.39	0.07
6c	390	3980	466	471	4180	0.39	0.28
6d	392	3590	474	482	4410	0.38	0.18
6e	390	4450	466	476	4180	0.36	0.52
6f	390	4110	467	478	4230	0.36	0.39
6i	398	4400	555	501	7110	0.19	0.18
6k	393	4100	480	479	6412	0.36	0.22
6m	398	4560	474	496	4130	0.42	0.27

[a] 10⁻⁵ M solution in CH₂Cl₂. [b] Absolute quantum yield measured with an integration sphere, solutions of **6** in PhCl (10⁻⁵ M) were purged with Ar for 20 min prior to measurement. [c] Absolute quantum yields measured with integration sphere.

As shown in Figure 6, the time-dependent DFT simulation under PCM(CH₂Cl₂)-TD-B3LYP/6-311+G(d,p) level of theory well represents the 'push-pull' character of **6a**. In the HOMO, the 4-phenyl group and the 3-hydroxy group communicate with the naphthalene backbone orbital (Figure 6A). On the other hand, the LUMO is mainly localized on the 1-hydroxy-2-naphthoate structure (Figure 6B).

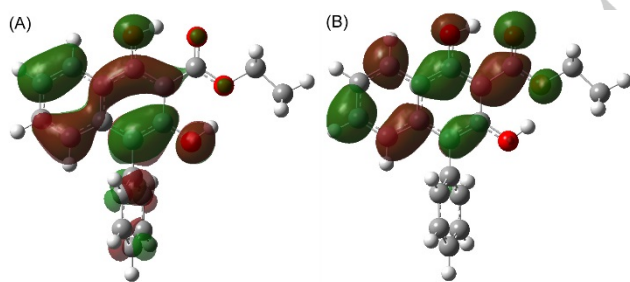
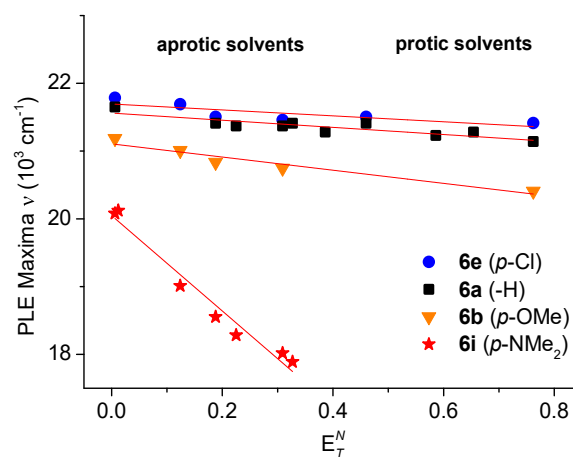


Figure 6. HOMO (A) and LUMO (B) of **6a** under PCM(CH₂Cl₂)-TD-B3LYP/6-311+G(d,p) level of theory with PCM (CH₂Cl₂).

Among the series of 4-phenyl naphthalenes, the *p*-(dimethylamino)phenyl derivative **6i** is a noteworthy exception: It shows a remarkable large Stokes shift of 7110 cm⁻¹ in CH₂Cl₂ (Table 2). In this case, **6i** after excitation most likely undergoes a TICT (twisted intramolecular charge-transfer) state that necessarily involves major changes in the molecular geometry of the vibrationally relaxed excited state. The TICT mechanism and

its electronic distribution in **6i** are likewise responsible for a significant PLE efficiency decrease in solutions.

Solvatochromism studies with **6a** (H), **6b** (*p*-OMe), **6e** (*p*-Cl), and **6i** (*p*-NMe₂) show significant bathochromic shifts of the PLE bands with Reichardt's normalized solvent polarity parameter E_T^N (Figure 7 and Supporting Information).^[24] Such a positive solvatochromism is indicative for an ICT originated from molecules having a donor-acceptor dyad. Notably, in these novel 'push-pull' structures, the acceptor ability is enhanced through a twofold intramolecular hydrogen bonding of the hydroxyl groups on the C1 and C3 atoms towards



FULL PAPER

Figure 7. PLE band maxima as a function of Reichardt's solvent polarity parameter E_{T}^{N} of compounds **6a**, **6b**, **6e** and **6i**.

the ester function on the C2 atom. This characteristic H-bonding also rigidifies the molecular structure being a reason for the observed high PLE quantum efficiencies (Table 2). Noteworthy to mention, these twofold H-bonds remain intact even in protic solvents like alcohols as being expressed by the fitting correlation of the band maxima ν_{max} of UV-Vis absorption and PLE spectra with the solvent polarity parameter E_{T}^{N} (Figure 7). Solution and solid state PLE spectra of **6** are quite similar with respect to their emission maxima and band shape with the notable exception of **6i** (see, Supporting Information for overlay of solution and solid state PLE spectra): Compared to the other examples in this series, the PLE band maxima of **6i** in chlorobenzene ($^{\text{em}}\lambda_{\text{max}} = 555 \text{ nm}$) is significantly red-shifted to that of the solid state ($^{\text{em}}\lambda_{\text{max}} = 501 \text{ nm}$). This again points to a favourable emission of **6i** through the TICT state in solutions.

Further insight into molecular structure and electronic properties of the excited state were gained from the Lippert-Mataga plots of **6a**, **6b**, **6d**, **6e-f**, and **6i** (Figure 8).

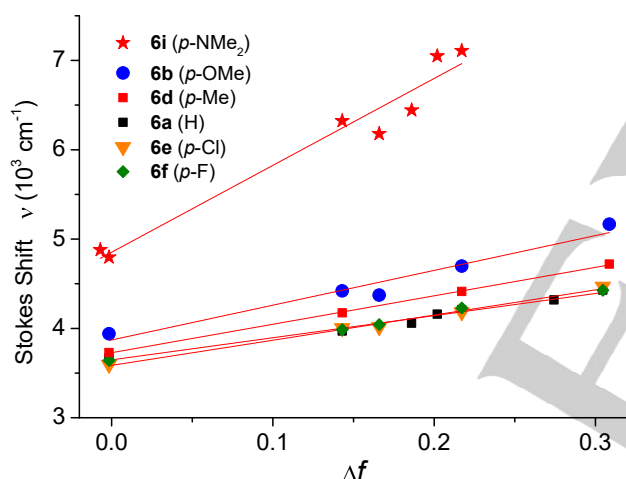


Figure 8. Lippert-Mataga plots of **6a**, **6b**, **6d**, **6e**, **6f** and **6i** as correlation of Stokes shift versus orientation polarizability Δf . Protic solvents were not considered.

Stokes shifts show a good correlation with Lippert's orientation polarizability Δf that quantifies the difference in polarization between the first excited and the ground states of a chromophore. It allows the estimation of the change of dipole moment for the transition from ground to the excited state (Supporting Information).^[25] Plotting Stokes's shifts vs $\Delta f = (\epsilon - 1)/(2\epsilon + 1) - (n^2 - 1)/(2n^2 + 1)$, where ϵ is the permittivity and n is the refractive index of the solvent, yield dipole moment changes between the ground (μ_g) and the excited (μ_e) states of 15.5, 15.9, 16.5, 17.6, 19.4, and 30.7 D for respectively **6a** (H), **6f** (p-F), **6e** (p-Cl), **6d** (p-Me), **6b** (p-OMe), and **6i** (p-NMe₂). For all investigated compounds **6** a solvent cavity (Onsager) radius of ca. 4.6 Å was estimated. This increase of $\mu_e - \mu_g$ in the set of **6a**, **6f**, **6e**, **6d**, **6b**, and **6i** again emphasizes on the ICT and 'push-pull' character originated by the interplay of donor strength variations by the substituents on the

C4-phenyl group and the naphthoate acceptor strengthened by the twofold intramolecular H-bonding.

HOMO/LUMO energy levels of **6a** and **6k** were investigated by a combination of cyclic voltammetry and the onset values of the low energy absorption bands (for details, see Supporting Information). Within the solvent/electrolyte window (0.1 M Bu₄NPF₆ in CH₂Cl₂), the parent compound **6a** and its 3-thienyl analogue **6k** show non-reversible oxidation half-waves with a first oxidation potential $E_{1/2}$ of 1.34 V and 1.22 V, respectively (Figure 9). From the onset of the first oxidation half-wave $^{\text{ox}}E_{\text{onset}}$ (1.19 V for **6a** and 1.13 V for **6k**) and the optical band gap $^{\text{opt}}E_{\text{gap}}$ (2.84 eV for **6a** and 2.09 eV for **6k**), that was taken from the onset of the UV-vis absorption spectra, the HOMO/LUMO energies were estimated to be -5.83/-2.99 eV (**6a**) and -5.77/-3.68 eV (**6k**).^[26]

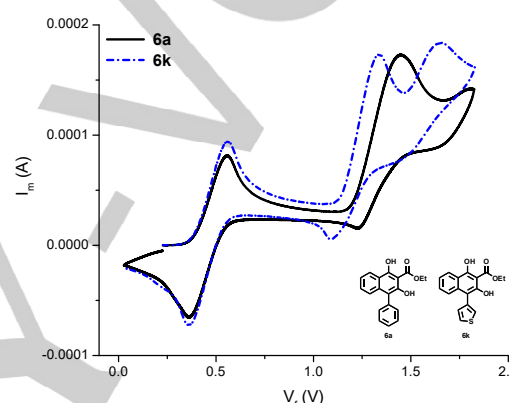


Figure 9. Cyclic voltammetry plot of **6a** and **6k** (10^{-3} M in CH₂Cl₂ / 0.1 M *n*-Bu₄NPF₆) at room temperature with internal Fc^{+/0}/Fc ($E_{1/2} = 0.46 \text{ V}$ vs SCE) for calibration purpose. Scan rate 100 mV/s, working electrode Pt, auxiliary electrode Pt wire, and the reference electrode SCE.

Conclusion

In conclusion, we successfully developed an effective route to less accessible 4-aryl-1,3-dihydroxy-2-naphthoates through a cascade reaction of brominated lactol silyl ethers including a sequential ring-opening/ring-closing process. The work illustrates that the bioinspired strategy is promising not only for natural product synthesis but also for discovering 'unnatural' polyaromatics with potent fluorescent properties characterised by 'push-pull' systems with ICT and TICT behaviour.

Experimental Section

General procedure for zwitterion-induced addition reaction: To a solution of halolactone **8** (0.5-3.0 mmol) and zwitterion **A** (1 mol%) in CH₂Cl₂, a solution of *tert*-butyl((1-ethoxyvinyl)oxy)dimethylsilane (KSA, 1.2-1.6 equiv) in CH₂Cl₂ (0.3 mL) was slowly added over 30-50 min by using a syringe pump at 0 °C. After being stirred additionally at the same temperature, the reaction mixture was quenched with a saturated NaHCO₃ aqueous solution (30 mL) and extracted with EtOAc (30 mL x 3). The combined organic layer was washed with brine (30 mL) and evaporated. Chromatographic purification of thus obtained residue was effective to isolate the desired lactol silyl ether **5**.

FULL PAPER

Ethyl 2-(4-bromo-1-((tert-butyldimethylsilyl)oxy)-3-phenyl-1H-isochromen-1-yl)acetate (5a-Br): According to the general procedure, this compound was obtained in 89% yield (1.35 g, 2.68 mmol) by the reaction of bromolactone **8a-Br** (904 mg, 3.00 mmol) with KSA (968 mg, 4.78 mmol) in the presence of zwitterion catalyst **A** (15.9 mg, 30.3 μ mol) in CH_2Cl_2 (15 mL). The KSA was added over 30 min at 0 °C, then the mixture was additionally stirred for 30 min at the same temperature. Isolation of the product was achieved by column chromatography on silica gel (hexane/EtOAc = 20 : 1). Colourless crystals (from hexane); IR (ATR) ν 2954, 2926, 2856, 1731, 1600, 1334, 1226, 1193, 1150, 1013, 836, 781, 753, 694 cm^{-1} ; ^1H NMR (400 MHz, CDCl_3) δ -0.15 (3H, s), -0.09 (3H, s), 0.89 (9H, s), 1.15 (3H, t, J = 7.2 Hz), 3.02 (1H, d, J = 13.6 Hz), 3.17 (1H, d, J = 13.6 Hz), 4.00-4.14 (2H, m), 7.33 (1H, td, J = 7.6, 1.2 Hz), 7.38-7.46 (5H, m), 7.60 (1H, dd, J = 7.6, 1.2 Hz), 7.85-7.90 (2H, m); ^{13}C NMR (100 MHz, CDCl_3) δ -3.7, -3.3, 14.0, 18.0, 25.7, 46.9, 60.6, 98.3, 100.9, 124.2, 124.9, 127.7, 127.8, 129.1, 129.3, 129.9, 130.0, 132.5, 134.4, 148.5, 168.4; HRMS (ESI-TOF) calcd for $\text{C}_{25}\text{H}_{31}\text{BrNaO}_4\text{Si}$ [$\text{M}+\text{Na}$] $^+$, 525.1073; found, 525.1071. Anal. Calcd for $\text{C}_{25}\text{H}_{31}\text{BrO}_4\text{Si}$: C, 59.64; H, 6.21. Found: C, 59.64; H, 6.20.

General procedure for the ring-rearrangement reaction: To a solution of lactol silyl ether **5** (0.2-0.5 mmol) in AcOH (0.1 mol L^{-1}), NaOAc (20 equiv) was added. After being stirred for 2.5-11 h at 70 °C, the reaction mixture was directly concentrated under reduced pressure. The resulting residue was dissolved in water (50 mL) and extracted with EtOAc (30 mL \times 3). The combined organic layer was washed with brine (30 mL) and evaporated. The resulting residue was purified by column chromatography on neutral silica gel eluting with hexane/EtOAc mixtures to give the desired 4-aryl-1,3-dihydroxy-2-naphthoate **6**.

Ethyl 1,3-dihydroxy-4-phenyl-2-naphthoate (6a): According to the general procedure, this compound^[15b] was obtained in 93% yield (71.2 mg, 0.231 mmol) by the reaction of lactol silyl ether **5a-Br** (125 mg, 0.248 mmol) in AcOH (2.5 mL) containing NaOAc (412 mg, 5.02 mmol) for 4 h at 70 °C and the following column chromatography on silica gel (hexane/EtOAc = 20 : 1). The molecular structure was also confirmed by single crystal X-ray structural analysis. Yellow crystals (from Et_2O); Mp. 123-124 °C; IR (ATR) ν 3407, 2923, 2853, 1656, 1635, 1400, 1297, 1232, 806, 771, 758, 697, 572 cm^{-1} ; ^1H NMR (400 MHz, CDCl_3) δ 1.51 (3H, t, J = 7.2 Hz), 4.63 (2H, q, J = 7.2 Hz), 7.32 (1H, ddd, J = 8.4, 6.4, 1.2 Hz), 7.34-7.39 (3H, m), 7.40-7.47 (2H, m), 7.49-7.55 (2H, m), 8.35 (1H, d, J = 8.4 Hz), 9.28 (1H, brs, OH), 11.61 (1H, brs, OH); ^{13}C NMR (100 MHz, CDCl_3) δ 14.2, 63.2, 97.0, 114.8, 119.5, 123.0, 124.1, 124.5, 127.2, 128.4, 130.4, 131.2, 136.0, 137.1, 150.1, 161.3, 170.3; HRMS (ESI-TOF) calcd for $\text{C}_{19}\text{H}_{17}\text{O}_4$ [$\text{M}+\text{H}$] $^+$, 309.1127; found, 309.1118. Anal. Calcd for $\text{C}_{19}\text{H}_{16}\text{O}_4$: C, 74.01; H, 5.23. Found: C, 73.75; H, 5.23.

One-pot synthesis of 6a: To a solution of 4-bromo-3-phenyl-1H-isochromen-1-one **8a-Br** (151 mg, 0.501 mmol) and zwitterion **A** (2.7 mg, 5.1 μ mol) in CH_2Cl_2 (2.2 mL), a solution of KSA (162 mg, 0.801 mmol) in CH_2Cl_2 (0.3 mL) was slowly added. After being stirred for 0.5 h at 0 °C, the reaction mixture was evaporated. Thus obtained residue was dissolved in AcOH (5.0 mL) and treated with NaOAc (820 mg, 10.0 mmol) for 4 h at 70 °C. After extractive workup and evaporation, the crude material was purified by column chromatography on silica gel (hexane/EtOAc = 15 : 1) to give the desired naphthalene **6a** in 95% yield (146 mg, 0.474 mmol) over two steps.

Acknowledgements

Financial supports by KAKENHI (20K06947), Japan, and the research cluster Labex EMC³ (energy materials and clean combustion center) and Région Normandie, France, are gratefully acknowledged.

Keywords: Synthetic methods • Domino reactions • Rearrangement • Polycycles • Fluorescence

- [1] J. Staunton, K. J. Weissman, *Nat. Prod. Rep.*, **2001**, *18*, 380.
- [2] J. Rohr, C. Hertweck, Type II PKS, in *Comprehensive Natural Products II*, Eds. H.-W. Liu and L. Mander, Elsevier: Amsterdam, 2010, Vol. 1, pp. 227-303.
- [3] For reviews, see: a) V. C. Fäseke, F. C. Raps, C. Sparr, *Angew. Chem. Int. Ed.*, **2020**, *59*, 6975; *Angew. Chem.*, **2020**, *132*, 7039; b) G. Genta-Jouve, S. Antoniotti, O. P. Thomas, Polyketide Assembly Mimics and Biomimetic Access to Aromatic Rings, in *Biomimetic Organic Synthesis*, Eds. E. Poupon and B. Nay, Wiley-VCH, 2011, Vol. 1, pp. 469-502.
- [4] F. Malpartida, D. A. Hopwood, *Nature*, **1984**, *309*, 462.
- [5] For selected examples, see: a) M. Harris, P. J. Wittek, *J. Am. Chem. Soc.*, **1975**, *97*, 3270; b) M. Harris, A. D. Webb, C. M. Harris, P. J. Wittek, T. P. Murray, *J. Am. Chem. Soc.*, **1976**, *98*, 6065; c) M. Yamaguchi, K. Shibato, I. Hiro, *Chem. Lett.*, **1985**, *14*, 1145; d) M. Yamaguchi, K. Hasebe, H. Higashi, M. Uchida, A. Irie, T. Minami, *J. Org. Chem.*, **1990**, *55*, 1611; e) T. N. Barrett, A. G. M. Barrett, *J. Am. Chem. Soc.*, **2014**, *136*, 17013.
- [6] a) Review, see: K. Krohn, *Eur. J. Org. Chem.*, **2002**, 1351; b) G. Bringmann, *Angew. Chem. Int. Ed. Engl.*, **1982**, *21*, 200; c) A. Link, C. Sparr, *Angew. Chem. Int. Ed.*, **2014**, *53*, 5458; *Angew. Chem.*, **2014**, *126*, 5562; d) R. M. Witzig, V. C. Fäseke, D. Häussinger, C. Sparr, *Nat. Catal.*, **2019**, *2*, 925.
- [7] H. Yanai, N. Ishii, T. Matsumoto, T. Taguchi, *Asian J. Org. Chem.*, **2013**, *2*, 989.
- [8] H. Yanai, N. Ishii, T. Matsumoto, *Chem. Commun.*, **2016**, *52*, 7974.
- [9] M. Garcia-Castro, S. Zimmermann, M. G. Sankar, K. Kumar, *Angew. Chem. Int. Ed.*, **2016**, *55*, 7586; *Angew. Chem.*, **2016**, *128*, 7712; (b) A. Garcia, B. S. Drown, P. J. Hergenrother, *Org. Lett.*, **2016**, *18*, 4852; (c) R. J. Rafferty, R. W. Hicklin, K. A. Maloof, P. J. Hergenrother, *Angew. Chem. Int. Ed.*, **2014**, *53*, 220; *Angew. Chem.*, **2014**, *126*, 224.
- [10] Selected examples for synthesis of 1,2,3,4-tetrasubstituted naphthalenes, see: a) J.-Y. Wang, P. Zhou, G. Li, W.-J. Hao, S.-J. Tu, B. Jiang, *Org. Lett.*, **2017**, *19*, 6682; b) G. Nares, R. Kant, T. Narendar, *Org. Lett.*, **2015**, *17*, 3446; c) B. S. Kale, R.-S. Liu, *Org. Lett.*, **2019**, *21*, 8434; d) T. Hamura, M. Miyamoto, T. Matsumoto, K. Suzuki, *Org. Lett.*, **2002**, *4*, 229.
- [11] Recent synthesis of 1,2,3,4-tetrasubstituted carbazoles, see: a) S. Singh, R. Samineni, S. Pabbaraja, G. Mehta, *Org. Lett.*, **2019**, *21*, 3372; b) T. N. Poudel, Y. R. Lee, *Chem. Sci.*, **2015**, *6*, 7028.
- [12] a) L.-Y. Chin, C.-Y. Lee, Y.-H. Lo, M.-J. Wu, *J. Chin. Chem. Soc.*, **2008**, *644*; b) S. Roy, S. Roy, B. Neuenswander, D. Hill, R. C. Larock, *J. Comb. Chem.*, **2009**, *11*, 1128.
- [13] H. Yanai, T. Yoshino, M. Fujita, H. Fukaya, A. Kotani, F. Kusu, T. Taguchi, *Angew. Chem. Int. Ed.*, **2013**, *52*, 1560; *Angew. Chem.*, **2013**, *125*, 1600.
- [14] H. Yanai, T. Taguchi, *Chem. Commun.*, **2012**, *48*, 8967.
- [15] a) K. Meyer, H. S. Bloch, *Org. Synth.*, **1945**, *25*, 73; b) J. Nieuwenhuis, J. F. Arens, *Rec. Trav. Chim. Pays Bas*, **1958**, *77*, 1153; c) E. M. O'Brien, B. J. Morgan, M. C. Kozlowski, *Angew. Chem. Int. Ed.*, **2008**, *47*, 6877; *Angew. Chem.*, **2008**, *120*, 6983; d) G. Wang, Y. He, J. Sun, D. Das, M. Hu, J. Huang, D. Ruhmund, L. Hooi, S. Misialek, P. T. R. Rajagopalan, A. Stoycheva, B. O. Buckman, K. Kossen, S. D. Seiwert, L. Beigelman, *Bioorg. Med. Chem. Lett.*, **2009**, *19*, 4476.
- [16] For reviews, see: a) S.-H. Wang, Y.-Q. Tu, M. Tang, The Semipinacol Rearrangement, in *Comprehensive Organic Synthesis II*, P. Knochel and G. A. Molander, Eds., Elsevier: Amsterdam, 2014, Vol. 3, pp. 795-852; b) Z.-L. Song, C.-A. Fan, Y.-Q. Tu, *Chem. Rev.*, **2011**, *111*, 7523.
- [17] Deposition Numbers 2011888 (**6a**), 2011882 (**6d**), 2011887 (**6f**), 2011881 (**6i**), 2011885 (**6j**), 2011883 (**6k**), 2011886 (**6m**), and 2011884 (**6p**) contain the supplementary crystallographic data for this paper. These data are provided free of charge by the joint Cambridge Crystallographic Data Centre and Fachinformationszentrum Karlsruhe Access Structures service www.ccdc.cam.ac.uk/structures.
- [18] a) *The Quantum Theory of Atoms in Molecules* (Eds.: C. F. Matta, R. J. Boyd), Wiley-VCH, Weinheim, **2007**; b) R. F. W. Bader, *Atoms in Molecules: A Quantum Theory*, Oxford University Press, Oxford, **1990**.

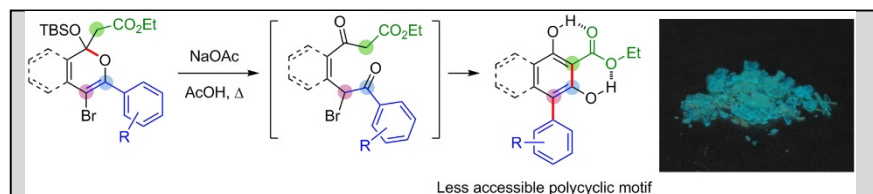
FULL PAPER

- [19] S. Mitra, A. K. Chandra, P. M. Gashnga, S. Jenkins, S. R. Kirk, *J. Mol. Model.* **2012**, *18*, 4225.
- [20] E. D. Glendening, F. Weinhold, *J. Comput. Chem.* **1998**, *19*, 593.
- [21] Compared to the tetrasubstituted derivatives, PLE quantum efficiency of methyl 1-hydroxy-2-naphthoate and methyl 2-hydroxy-3-naphthoate is known to be much lower, see: J. Catalán, J. C. del Valle, J. Palomar, C. Díaz, J. L. G. de Paz, *J. Phys. Chem. A*, **1999**, *103*, 10921.
- [22] C. Hansch, A. Leo, R. W. Taft, *Chem. Rev.*, **1991**, *91*, 165.
- [23] For ICT mechanism in 2,6-disubstituted biaryl systems, see: (a) A. J.-T. Lou, T. J. Marks, *Acc. Chem. Res.*, **2019**, *52*, 1428; (b) S. Sasaki, Y. Niko, A. S. Klymchenko, G. Konishi, *Tetrahedron*, **2014**, *70*, 7551.
- [24] C. Reichardt, *Solvents and Solvent Effects in Organic Chemistry*, 3rd Ed., Wiley-VCH: Weinheim, 2003.
- [25] a) E. Lippert, *Z. Naturforsch. A.*, **1955**, *10*, 541; b) H. Beens, H. Knibbe, A. Weller, *J. Chem. Phys.*, **1967**, *47*, 1183.
- [26] H. Srour, T.-H. Doan, E. Da Silva, R. J. Whitby, B. Witulski, *J. Mater. Chem. C*, **2016**, *4*, 6270.

FULL PAPER

Entry for the Table of Contents

Insert graphic for Table of Contents here.



Under gentle heating conditions in NaOAc/AcOH, brominated lactol silyl ethers were selectively converted to 4-aryl-1,3-dihydroxy-2-naphthoates – a naphthalene scaffold with a fully substituted benzene unit. The present reaction including a 1,2-aryl migration process was successfully applied to construct a wide range of polycyclic systems including biphenyl, anthracene, and benzothiophene structures. In addition, the 4-aryl-1,3-dihydroxy-2-naphthoate products showed bright photoluminescence emission from solid-state as well as in several organic solvents.